Rare-earth element minerals in four carbonatites near Gatineau, Quebec

Donald D. Hogarth, Ron Hartree, John Loop

Ottawa-Carleton Centre for Geoscience Studies
Department of Geology, University of Ottawa
Ottawa, Ontario, Canada K1N 6N5

and Todd N. Solberg

Department of Geological Sciences
Virginia Polytechnic Institute and State University
Blacksburg, Virginia 24061

Abstract

Near Gatineau, Quebec lens-shaped and vein-form carbonatites cut Precambrian fenitized biotite gneiss and quartzite. Major minerals are calcite, barite, fluorapatite and hematite and variable amounts of celestite, dolomite, strontianite, aegirine, magnesio-arfvedsonite, microcline, albite, phlogopite, fluorite, rutile, quartz, monazite and REE fluocarbonates.

The carbonatites are distinctly rich in magnesium (0.3–12.2 wt.% MgO) manifest by silicates in the veins and silicates and/or ankerite in the lenses. They are also high in lanthanides (La + Ce + Nd + Gd + Er + Yb from 370 to 41000 ppm), strongly enriched in LREE (La/Yb ratios ranging from 69 to 1000) and high in barium (2.7–19,8 wt.% BaO). The BaO/SrO ratios vary between 0.9 and 66.

Where phosphates are the sole important lanthanide bearers, fluorapatite contains 1.2–1.7 wt.% Ce_2O_3 (similar to apatite in nearby fenite), where associated with REE fluocarbonate, it contains 0.25 to 0.35 wt.% Ce_2O_3 only, but with concomitant increase in the bulk-rock cerium. Ce-rich apatite appears to be primary and relatively unaltered but the Ce-poor apatite is either leached or secondary. Parisite and synchysite formed in situ through the breakdown of apatite, and unidentified REE fluocarbonates were deposited from solution after leaching and transportation.

Mineral association and compositions suggest low temperature and strong oxidation. Calcite and dolomite equilibrated at 240–300°C. It is suggested that emplacement was hydrothermal and controlled by faults of the Ottawa-Bonnechere rift system.

Introduction

Lanthanide-rich carbonatites have been noted in various world-wide localities (e.g., Mountain Pass, California, Glenover, South Africa; south Gobi Desert, Mongolia) yet, compared with their niobium-rich counterparts, they are poorly understood. This paper describes four carbonatites in order to put a new locality on record and to trace the development of rare-earth element (REE) minerals in carbonatites of a specific locale. The term carbonatite is used in the broad sense of Heinrich (1966, p. 13) who defines it as "a carbonate-rich rock of apparent magmatic derivation or descent", thereby including both magmatic and hydrothermal types. Comparison will be made with two apatite-rich lenses in fenite.

The carbonatites lie within a belt, approximatly 4 km wide (Fig. 1), which extends from near the city of Gatineau, Quebec, at least 22 km north-northeast. Within this belt, scattered fenites characterized by magnesio-arfvedsonite, aegirine, sodic phlogopite, microcline, albite, fluorapatite,

calcite and barite replace regionally metamophosed (Grenville) gneiss and quartzite and, themselves, give late Grenvillian (ca. 900 m.y.) K–Ar ages. The pyriboles have been progressively enriched in sodium during their development (Hogarth and Lapointe 1984).

Interspersed through the fenites are a few small carbonatites (Hogarth 1981). These rocks are weakly to strongly layered parallel to their walls due to alternating dolomite and calcite, dolomite and barite or calcite and barite fractions. Some are concordant with the regional foliation but others are clearly discordant. A calcite–barite–apatite–hematite association is common to all occurrences. In the larger bodies (sites 2 and 3, Fig. 1), carbonatites pass transitionally into country rock as breccia, then into calcite-sealed fractures and, finally, into solid rock. The xenoliths and wall rocks are normally strongly fenitized.

The region is cut by gravity faults of the Ottawa-Bonnechere rift structure, important to the emplacement of alkaline rocks and carbonatites in Ontario and Quebec and which are known to have been rejuvenated period-

ically since late Precambrian time (Kumarapeli and Saull 1966; Lumbers 1978).

Methods of investigation

Whole rock analyses

Most elements, were determined (RH analyst) by XRF on lithium borate glasses with a rhodium tube, operated at 60 kV and 40 mA. La, Ce, Nd, Gd, Er, and Yb were determined (JL analyst) by a special procedure which involved combined multi-acid/LiBO$_4$ dissolution followed by separation in a cation-exchange column. The REE fraction was determined with a direct current plasma-atomic emission spectrophotometer (DCP-AES). Standards were specially prepared aqueous solutions, controls were various international rock standards. Precision was determined as: La 2, Ce 3, Nd 3, Gd 2, Er 8, Yb 14%. The precision of Y (XRF analysis) was estimated at 10%. In two samples, uranium was determined by delayed neutron counting (DNC; X-ray Assay Laboratories analysts).

For compositions of carbonatite rocks given in Table 1, the balance in total can be assumed to be mainly CO$_2$ and H$_2$O, which were not determined in our analyses.

Mineral analysis

Polished thin sections, first examined visually, were excited to cathodoluminescence (CL) with an electron beam following the procedure of Mariano and Ring (1975), in order to isolate potential areas for microprobe work. Most microprobe analyses were made at Virginia Polytechnic Institute (by DDH and TNS) with an ARL–SEMQ, 9-channel microprobe following the analytical procedures outlined by Solberg (1982) and Solberg and Speer (1982). Backgrounds for REE were particularly difficult to determine due to spectral interferences and, therefore, were carefully chosen. Overlapping peaks were subtracted in a procedure similar to that outlined by Wayne (1984). REE standards were synthetic La-V oxide, Ce oxide, Nd$_2$Si$_2$O$_7$ (Speer and Solberg 1982), Nd$_3$Ga$_5$O$_{12}$ and Y-Al garnet. Actinide standards were synthetic UO$_2$, U-bearing glass (XGL) and Th-bearing glass (WGL). Other standards were natural or synthetic phases as quoted in Solberg (1982) and Solberg and Speer (1982). Arsenic in apatite H was determined by a detailed spectral scan and compared with Durango apatite. Automated traverses (19 elements analyzed) were made across specimens A, E and I.

Some specimens were analyzed at Carleton University by Peter Jones, using a Cambridge Geoscan Mk 5 microprobe operated with an accelerating voltage of 15 kV, a beam current of 10 nA, and a 10 μm beam width. In apatite, La, Ce, Pr and Nd were determined with the REE-bearing glass standards described by Drake and Weill (1972) and overlapping peaks were subtracted by the method of Åmli and Griffin (1975). For monazite, the following REE standards were used: LaAlO$_3$, CeO$_2$ REE glasses (Pr, Nd, Y). Th was determined with Th metal; U with synthetic brannerite; Ca, P, F with Durango apatite; Fe, Si with Kakanui hornblende; S, Sr with natural celestite. Data were reduced using the EMPADR program of Rucklidge and Gasparrini (1969).

Description of occurrences and specimens

The four carbonatites and two fenites are located on Figure 1. The following description summarizes essential features of geology and mineralogy.

Site 1

Fenite contains a few carbonatite veins, the largest being 0.25 m thick. The principal pyribole of the fenite is magnesio-arfvedsonite
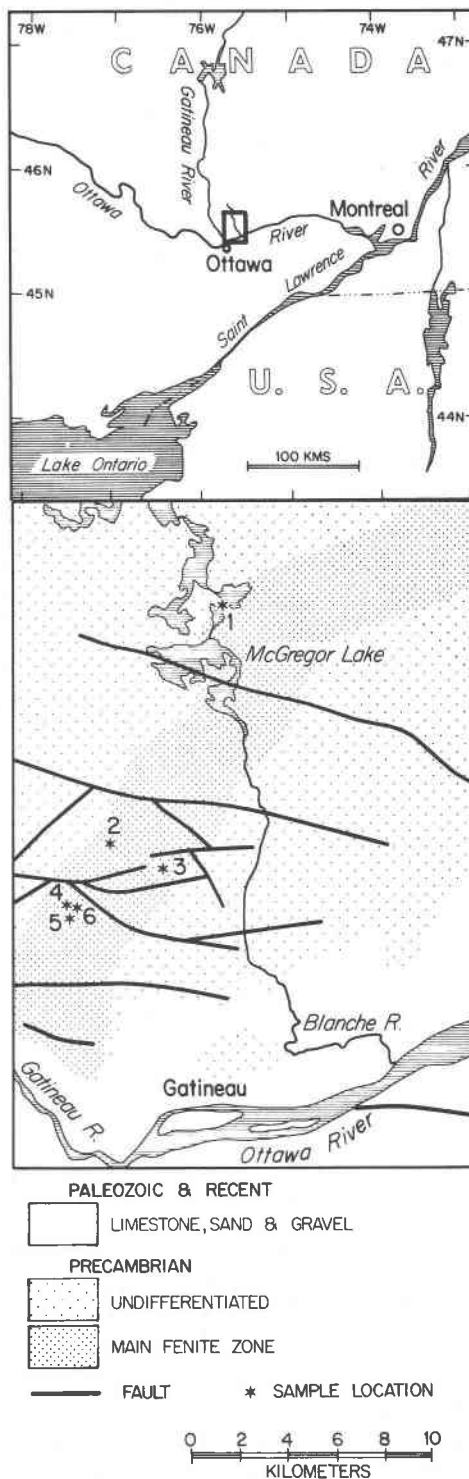

Fig. 1. Map showing location of occurrences.

but, near carbonatite, aegirine becomes dominant. Carbonatite is composed of coarse calcite with local concentrations of aegirine, magnesio-arfvedsonite, barite, monazite, rutile and hematite.

Two specimens (A and B), each from a separate vein, are composed as follows: (A) 60% coarse pink calcite, 25% strontian

Table 1. Whole-rock chemical analyses

Site	1		2				3		4
Sample	A	B	C	D	E	F	G	H	I
SiO$_2$ %*	8.81	0.52	11.70	20.58	11.04	6.61	0.68	4.87	19.50
TiO$_2$	0.28	0.03	0.15	0.24	0.17	0.11	0.09	0.09	0.60
Al$_2$O$_3$	0.41	0.04	2.68	2.83	2.06	1.14	0.17	0.09	1.05
FeO$_T$	2.74	0.29	2.40	7.10	2.73	2.38	6.71	0.75	8.51
MnO	0.09	0.55	0.20	0.28	0.19	0.28	0.39	0.21	0.31
MgO	0.80	0.26	4.99	4.54	4.70	4.42	12.17	14.16	1.64
CaO	26.47	48.59	33.17	24.59	35.37	39.37	25.71	24.41	24.32
BaO	19.78	3.13	2.70	4.32	5.52	5.28	10.50	10.87	4.85
SrO	0.78	3.35	0.26	3.08	0.90	0.42	0.16	0.25	0.65
Na$_2$O	1.34	0.21	0.22	2.53	0.33	0.06	0.07	0.06	0.07
K$_2$O	0.10	0.01	1.80	2.02	1.45	0.77	0.00	0.00	0.18
P$_2$O$_5$	0.30	0.42	0.96	1.64	0.88	0.59	1.01	1.22	0.62
SO$_{3T}$	9.51	1.82	1.25	3.65	3.17	2.77	4.34	4.92	2.62
Y ppm	25	33	65	58	93	92	192	186	155
La	83	106	672	792	645	333	1260	1612	9405
Ce	190	231	1410	1750	1350	915	2600	3125	22100
Nd	85	104	475	642	522	478	1032	1128	8925
Gd	12	14	32	36	36	40	90	98	192
Er	1.9	2.7	6.7	6.1	7.4	7.8	14.0	13.6	11.0
Yb	1.2	1.4	4.9	3.9	5.5	6.7	9.6	8.8	9.0
ΣLn **	373	459	2600	3230	2570	1780	5010	5990	40600
La/Nd	0.98	1.02	1.41	1.23	1.24	0.70	1.22	1.43	1.05
La/Yb	69	75	140	200	120	50	130	180	1000

* Y and elements listed as oxides analyzed by XRF. Lanthanides determined by DCP.

** ΣLn = La + Ce + Nd + Gd + Er + Yb.

barite, 10% aegirine, 1% (fluor) magnesio-arfvedsonite, 1% fluorapatite and minor rutile and monazite. (B) 90% coarse, yellowish calcite, 5% barite, 5% celestite, 1% aegirine, 1% fluorapatite and minor rutile.

Site 2

A lens-shaped carbonatite crops out as a small (150 sq. m) knob of rock, projecting 8 m above the overburden. One contact with fenitized gneiss and granite pegmatite is exposed and intensely fenitized xenoliths are distributed profusely through the rock. The carbonatite is stained brown with iron oxides.

The four samples from site 2 (C to F) have 70–90% calcite, 10–20% (fluor) phlogopite, 5–10% barite (commonly intergrown with celestite) and 1 to 3% fluorapatite. Niobium-free rutile was present in all four specimens and dolomite-ankerite was present in two specimens (D and F). The following additional silicates, some of which may represent fenitized xenoliths, were identified in samples C and D: zones (fluor) magnesio-arfvedsonite, zoned aegirine, microcline (Or 98.0, Ab 1.8, Cn 0.2, An 0.0) and albite (Ab 99.3, Or 0.7, An 0.0). Under the cathodoluminoscope, albite luminesces a brilliant red, indicating Fe^{3+} activation, a feature prevalent in albite from carbonatites and fenites (Mariano 1978).

Site 3

This lens-shaped carbonatite is exposed along the side of a hill for a length of 275 m. A poorly developed fenite is marked by intense hematite staining and abundant barite–calcite–rutile veinlets at the contact. Carbonatite is yellow brown to brick red, contains abundant dolomite and barite, variable calcite and fluo-

Table 2. Microprobe analyses of apatite

| Site	1		2				3		4		5	6
Sample	A	B	C	D	E	F	G	H	I	J	K	L
UO$_2$	0.01	0.00	0.02	0.02	0.01	0.01	0.03	0.00	0.02	----	----	----
ThO$_2$	----	----	0.00	0.00	0.00	0.00	----	----	0.01	----	----	----
La$_2$O$_3$	0.59	0.52	0.51	0.54	0.67	0.78	0.04	0.13	0.06	0.12	0.52	0.38
Ce$_2$O$_3$	1.72	1.39	1.28	1.22	1.41	1.46	0.26	0.33	0.28	0.30	1.29	0.87
Pr$_2$O$_3$	----	----	----	----	----	----	----	----	----	0.03	0.18	0.07
Nd$_2$O$_3$	1.01	0.78	0.64	0.58	0.72	0.68	0.22	0.24	0.28	0.16	0.62	0.40
Y$_2$O$_3$	0.04	0.05	0.02	0.01	0.02	0.03	0.11	0.05	0.06	----	----	----
FeO$_T$	0.02	0.02	0.02	0.02	0.02	0.02	0.15	0.01	0.01	0.13	0.14	0.14
MnO	0.04	0.05	0.04	0.05	0.05	0.04	0.07	0.05	0.05	0.13	0.13	0.16
BaO	0.04	0.05	0.03	0.01	0.02	0.00	0.05	0.03	0.01	----	----	----
SrO	3.75	3.81	4.94	4.98	4.98	5.04	0.07	0.62	4.09	4.32	3.74	6.18
CaO	49.31	48.37	48.60	48.89	46.48	47.75	54.58	54.61	52.40	51.28	49.92	49.38
Na$_2$O	0.74	0.68	0.58	0.55	0.65	0.70	0.10	0.08	0.20	0.07	0.50	0.30
SO$_3$	0.17	0.06	0.10	0.11	0.18	0.20	0.08	0.07	0.05	0.07	0.16	0.13
P$_2$O$_5$	40.26	40.20	40.36	40.88	41.16	38.65	39.67	39.77	40.21	40.72	39.24	40.46
SiO$_2$	0.02	0.01	0.02	0.00	0.04	0.00	0.04	0.04	0.00	0.00	----	----
V$_2$O$_5$	----	----	0.02	0.02	0.01	0.01	----	----	0.02	----	----	----
As$_2$O$_5$	----	----	----	----	----	----	----	----	0.03	----	----	----
F	3.56	3.70	3.45	3.65	3.80	3.43	3.50	3.44	3.38	3.62	3.31	3.78
Cl	0.00	0.01	0.00	0.00	0.00	0.00	0.02	0.00	0.00	0.00	0.01	0.00
	101.28	99.70	100.64	101.53	100.23	98.82	98.99	99.47	101.13	100.95	99.76	102.25
O=F,Cl	1.50	1.56	1.45	1.54	1.60	1.44	1.47	1.45	1.42	1.52	1.39	1.59
Total	99.78	98.14	99.19	99.99	98.63	97.38	97.52	98.02	99.71	99.43	98.37	100.66
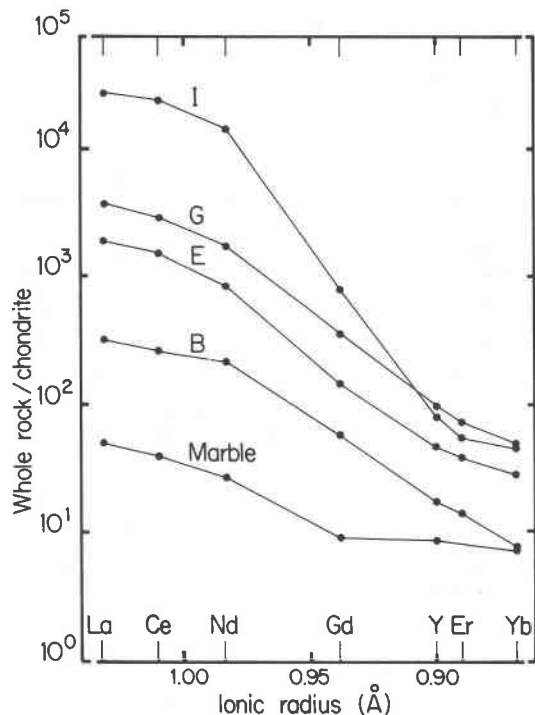
Fig. 2. Chondrite-normalized REE + Y abundances of typical samples and the average Grenville marble of Shaw et al. (1976). Chondrite values were taken form Haskin et al. (1968) and ionic radii from Shannon (1976).

rite but, other than sporadic quartz and very rare microline, totally lacks silicates.

Grains tended to be small, have irregular borders and are riddled with inclusions. Of 22 specimens studied, two only (G and H) proved suitable for detailed microprobe study. G contains about 70% coarse dolomite-ankerite, 25% calcite and 5% apatite + fluocarbonates. Apatite is present as wisps and tiny rounded crystals, fluocarbonate as a myriad of paper-thin veinlets. H is similar but contains about 5% quartz, some of which is in direct contact with dolomite.

Site 4

The carbonatite vein is bordered by a well developed aegirine fenite. The hanging wall is a calcite–barite–parisite layer, up to 1.3 m thick, the foot wall is a calcite–barite–specularite–aegirine layer, about 1 m thick.

Specimen I, representing the calcite–barite–parisite association, was selected from a part of the vein particularly rich in pink barite (10%), associated with parisite (10%) and synchysite (2%). Fluorapatite constitutes 1%.

Apatite sample J (Table 2) comes from a calcite–barite–specularite–aegirine association. The rock contains coarse-grained calcite (50%) cut by an interconnecting network of barite (30%) associated with specularite (10%), fluorapatite (5%), parisite and aegirine (1%). Specularite contains an intergrown (exsolution?) trellis of rutile.

Sites 5 and 6

These are small (up to 0.5 m across), lens-like accumulations within fenite. Apatite, specularite and phlogopite are the major constituents but the relative proportions of one mineral to the

other varies greatly, even within small adjoining areas. The rocks were, therefore, not analyzed. Monazite is minor (about 1 vol.% in specimen K, 0.5 vol.% in specimen L). Specularite contains an intergrowth trellis of rutile.

Geochemistry

Whole-rock analyses are given in Table 1. Notably, the carbonatites are rich in Ba, S, light REE (LREE) and Mg, variable in Sr, but poor in Nb (≤ 10 ppm by XRF) and U (0.75 and 8.0 ppm by DNC in samples C and G, respectively). Barium is present mainly in barite and celestite; it is comparatively insignificant in phlogopite and feldspar. Sulfur is present principally in sulfates since the samples contain virtually no sulfides.

Strong enrichment in LREE, especially sample I, can be seen from the chondrite-normalized chart of Figure 2. This distribution is similar to those in carbonatites from other regions (see, for example, the distributions given by Samoylov and Smirnova 1980). A Grenville marble trend is shown for comparison. REE are present as fluocarbonates and phosphates.

In common with REE carbonatites from many worldwide localities, the Gatineau carbonatites from sites 2, 3, and, to a lesser extent, sites 1 and 4, are rich in magnesium. The high-Mg content of lens-shaped bodies vs. lower Mg content of veins has been noted in additional occurrences discovered during the summer of 1984 and, apparently, characterizes carbonatites of this region. The magnesium is incorporated in silicates in the vein carbonatites (sites 1 and 4), or as dolomite-ankerite $\pm$ silicates in the lens carbonatites (sites 2 and 3).

Phosphates and carbonates

Apatite

All analyzed grains were lanthanide-bearing fluorapatite. Crystals from sites 1 and 2 were long prismatic, those from sites 4, 5, 6 were short prismatic to rounded anhedral, and those from site 3 were rounded to irregular. Grains cathodoluminesced blue due to Eu^{2+} activation (Mariano and Ring 1975). Notable is high strontium (4–7% SrO) in apatite from three of the four carbonatites and from fenite. "Average" compositions, derived from several analyses on especially clean portions of grains, are listed in Table 2.

Apatite from sites 1, 2, 4, 5 and 6 is rich in strontium; that from site 3 (samples G, H and two other specimens analyzed) contains a relatively low strontium concentration. Rare, zoned grains in specimens from sites 1 and 2 show a somewhat higher Sr concentration in the core than on the rim.

Some crystals show a Ce-rich zone near the edge. This feature is well marked in apatite from sites 1, 2, 5 and 6, less well marked in apatite from site 4 and was not observed in apatite from site 3.

Figure 3 illustrates a smooth, chemical variation in a typical zoned apatite grain. The traverse was made across the grain from the edge *a*, through a barite-bearing fracture *b*, to the opposite edge *c*. Nd, La and Y mimic Ce trends with $Ce_2O_3 : Nd_2O_3 : La_2O_3 : Y_2O_3 = 1 : 0.47 : 0.45 : 0.02$.
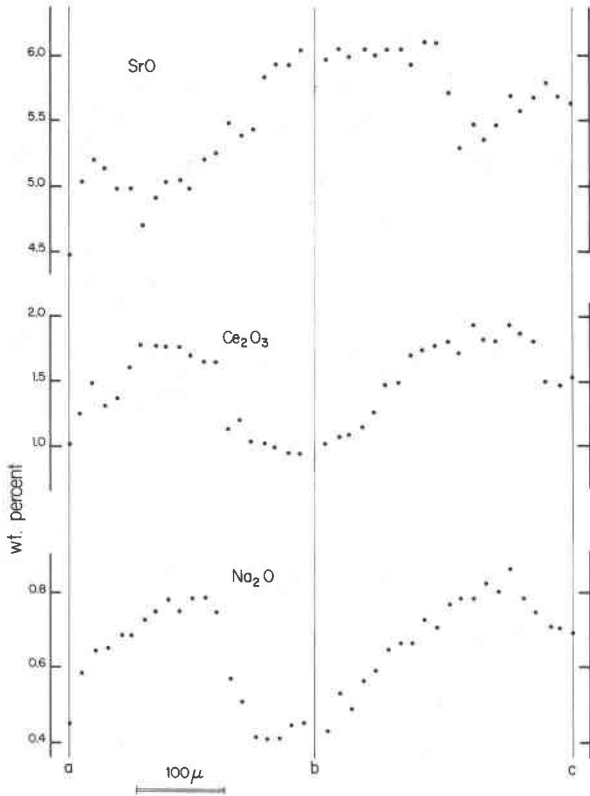
Fig. 3. Microprobe traverse across a grain of apatite in sample E. Line *b* locates a fracture.
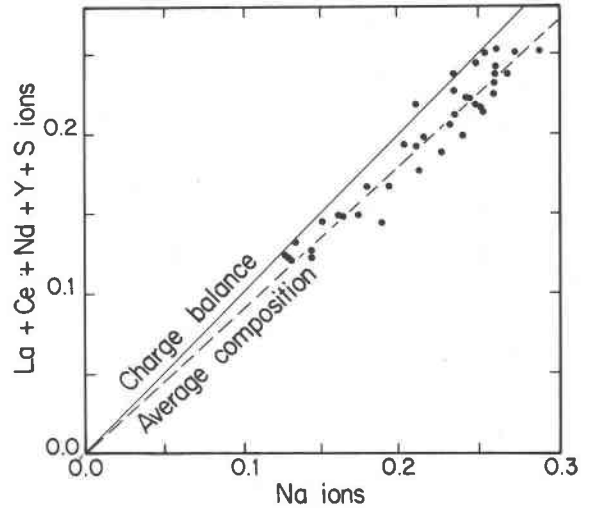

Fig. 4. Charge-balance diagram for the apatite grain of Figure 3. Cations are based on 50 positive charges in the chemical formula. The "average composition" represents a line drawn through the origin and the mean.

Monazite

Monazite occurs as large euhedral grains, closely associated with apatite (sites 1 and 2) and tiny rounded grains, interstitial in apatite (sites 5 and 6). An analysis of monazite (site 5, sample K) is presented in Table 3. The grains are rounded with Th concentrated on the rims. The zoning
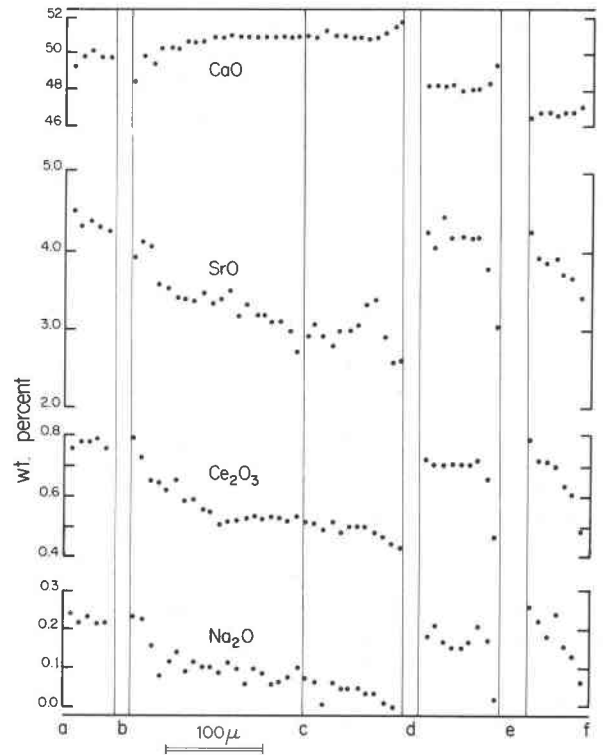
Anomalous values at *b* have been omitted from the illustration.

The additional charge resulting from REE^{3+}, Y^{3+} and S^{6+} is 90% compensated according to the substitution schemes:

$$Ca + Ca \rightarrow Na + REE, Y$$

$$Ca + P \rightarrow Na + S$$

The charge balance is illustrated in Figure 4. The remaining 10% charge imbalance is probably due to other REE, not determined.

Many crystals (all occurrences) are cut by intersecting fractures, with neighboring fracture-bounded segments abruptly mismatching in Sr and Ce. Figure 5 is a typical examle. The traverse was run from *a*, close to the edge, lengthwise across the grain to *f*, on the opposite edge. Lines *b*, *d* and *e* are fractures, partly filled with barite and REE fluocarbonate; *c* is a minor unfilled fracture. Chemical discontinuities are evident at *d* and *e* and perhaps *b* and *c*. For simplicity, anomalous values within the fractures have been omitted from the illustration.

The genetic significance of these variations cannot be established with certainty, but the marked, rather symmetrical and repetitive zoning of Figure 3 may represent growth pattern whereas the mismatched segments in Figure 5 probably represent leaching and addition of elements, guided by fracture patterns or, simply, secondary alteration.

Fig. 5. Microprobe traverse along the length of a grain of apatite in sample I. Lines b, c, d, e represent fractures.

Table 3. Microprobe analyses of unidentified carbonate (G(1), G(2)), parisite (I) and monazite (K)

Site	3		4	5	Formulae*			
Sample	G(1)	G(2)	I	K		I		K
UO_2	0.02	0.02	0.00	0.00	U	0.000	U	0.000
ThO_2	0.00	0.00	0.00	0.23	Th	0.000	Th	0.002
La_2O_3	13.67	9.67	13.72	20.56	La	0.442	La	0.301
Ce_2O_3	28.86	22.61	27.08	35.10	Ce	0.866	Ce	0.510
Pr_2O_3	----	----	----	4.20	Nd	0.350	Pr	0.061
Nd_2O_3	7.02	5.70	11.21	10.70			Nd	0.152
					Y	0.008	Ca	0.003
Y_2O_3	0.42	0.56	0.17	0.00	Al	0.001	Σ	1.03
Al_2O_3	0.06	0.07	0.01	0.00	Fe	0.019		
FeO_T	10.82	12.57	0.26	0.00	Mn	0.000	Si	0.006
MnO	0.01	0.00	0.00	----	Mg	0.033	P	0.978
MgO	0.14	0.20	0.25	----	Σ	1.72	Σ	0.98
BaO	0.03	0.19	0.00	----	Ba	0.000		
SrO	0.34	0.65	1.29	----	Sr	0.065		
CaO	14.85	14.87	9.93	0.06	Ca	0.929		
Na_2O	0.08	0.08	0.00	----	Na	0.000		
K_2O	0.04	0.04	0.05	----	K	0.006		
					Σ	1.00		
P_2O_5	0.00	0.00	0.00	29.14				
CO_2*	----	----	25.16	----	F	1.950		
SiO_2	0.00	0.00	0.00	0.16	Cl	0.003		
						1.95		
F	3.41	3.47	7.06	----				
Cl	0.06	0.10	0.02	----				
Total	78.38	69.32	93.28	100.15				

* Sample I, calculations based on 1 atom Ba + Sr + Ca + Na + K. CO_2 calculation based on 3 atoms C. Sample K, calculations based on 4 atoms O.
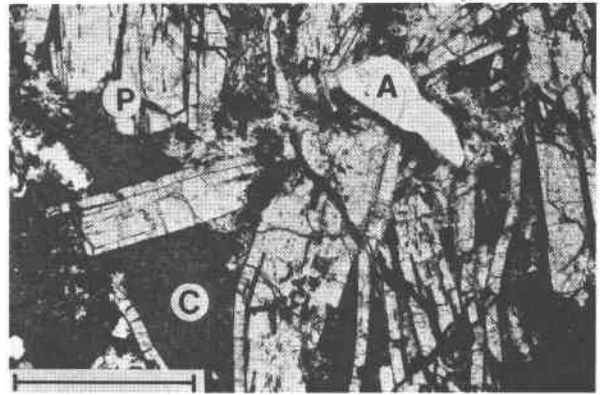

Fig. 6. Photomicrograph of tabular parisite (P), rounded apatite (A) and interstitial calcite (C). Sample I, plane-polarized light, calcite stained with alizarin. Bar scale represents 1 mm.

Calcite, dolomite, ankerite and strontianite

Compositions of calcite and dolomite are reported in Table 4. Ce_2O_3 in amounts of 0.02 and 0.03% must be regarded as at the limit of detection and even values of 0.07% (6–8 analyses, 20 sec counts) are subject to 50% error. However, these low values do show that calcite and dolomite are not enriched in REE. It is also evident that Sr, commonly reported in amounts $\geq 2\%$ in calcite from carbonatites, is (with the exception of sample J) comparatively low in the Gatineau specimens. Furthermore, the calcite contains little Mg, even when associated with dolomite. It does, however, contain appreciable amounts of Mn.

Dolomite-ankerite is locally important at site 2 and is the dominant mineral at site 3. At the latter site, early-formed dolomite (sample G(1), Table 4) is comparatively poor in Fe, but rich in Mn. Some crystals show rhythmic growth with calcite and take the form of large, composite rhombohedra. This early dolomite is transected by low-Mn ankerite veinlets (G(2)).

Specimen D contained an unusual dolomite, which consistently gave high Sr values on the VPI probe. A repeat analysis by Peter Jones on the Carleton probe produced almost identical results. The $L\alpha$ image showed Sr homogeneously distributed within the dolomite. With respect to surrounding calcite, it is strongly partitioned into the dolomite.

In specimens G and H, some calcite contained small grains of strontianite showing the characteristic blue Eu^{2+} CL. Apatite in the same section was virtually non-luminescent and suggests that Eu^{2+} is preferentially parititoned into strontianite rather than apatite, although these minerals may represent different generations. Considering the highly oxidized nature of these rocks (occurrence of aegirine, hematite, and the hematite-rutile association), it is indeed surprising that appreciable europium should be in the divalent state. Similar partitioning of Eu^{2+} in strontianite from the Bouga carbonatite, Angola, was described and illustrated by Mariano (1978).

is also expressed as bright blue CL on the rims of crystals, suggesting Eu^{2+} activation. No La, Ce, Pr or Nd zoning was observed.

The REE distribution in sample K is normal and closely resembles monazite from alkalic rocks and carbonatites (Fleischer and Altschuler 1969) except for above-normal values of Nd. The mineral appears to be more La-selective (with respect to other REE) than the associated apatite.

Rare earth fluocarbonates

Parisite (Table 3, specimen I) and synchysite were confirmed by X-ray diffraction. Euhedral, tabular crystals of parisite, up to 2 mm along the base, are closely associated with barite (Fig. 6). Surrounding many crystals is a fine-grained accumulation of synchysite. Zoning was not detected in these minerals.

The main REE mineral at site 3 appears to be a cerian fluocarbonate, occurring as paper-thin veinlets in calcite and dolomite. A widening of one of these veinlets permitted two analyses (G(1) and G(2), Table 3), which did not lead to a rational chemical formula. An iron image suggested impurity. The analyses may therefore represent one or more REE fluocarbonates and hematite.

Table 4. Microprobe analyses of calcite and dolomite-ankerite

| Site | Calcite | | | | | | | | | | Dolomite – Ankerite | | | |
| | 1 | | 2 | | | | 3 | | 4 | | 2 | 3 | | |
Sample	A	B	C	D	E	F	G	H	I	J	D	G(1)	G(2)	H
Ce_2O_3	0.07	0.02	0.03	0.03	0.02	0.02	0.04	0.05	0.03	0.00	0.00	0.03	0.00	0.03
FeO	0.13	0.53	0.16	0.24	0.14	0.08	0.15	0.10	0.39	0.62	7.23	1.41	7.80	0.73
MnO	0.57	0.76	0.73	0.58	0.40	0.40	0.60	0.52	0.76	1.12	1.23	0.81	0.30	0.50
MgO	0.07	0.19	0.08	0.16	0.49	0.21	0.23	0.48	0.24	0.32	16.60	20.62	16.44	20.87
CaO	55.30	54.50	54.31	53.97	55.57	54.27	55.71	54.96	55.29	52.44	28.66	29.49	29.52	29.88
BaO	0.03	0.02	0.03	0.03	0.00	0.04	0.00	0.03	0.03	0.14	0.00	0.00	0.00	0.04
SrO	0.32	0.27	0.26	0.27	0.10	0.14	0.09	0.26	0.34	0.98	1.28	0.00	0.00	0.06
CO_2*	44.07	43.90	43.39	43.17	44.53	43.19	44.48	44.17	44.52	43.03	46.35	47.03	46.08	47.04
Total	100.56	100.19	98.99	98.45	101.25	98.35	101.30	100.57	101.60	98.65	101.35	99.39	100.14	99.15

* Calculation based on CO_3: cations = 1 : 1

Origin

The absence of associated alkaline rocks, absence of a large, central carbonatite, but the overwhelming dominance of fenites, are not features typical of carbonatites. However, these features do characterize some carbonatites elsewhere, such as those at Wigu Hill, Tanzania (Heinrich 1966) and near the Great Glen Fault, Scotland (Garson et al. 1984). The Gatineau rocks are believed to be REE-barite carbonatites. The rifted platform environment, cross-cutting relationships, association with well developed fenites, high REE content (400 to 40,000 ppm), dominance of LREE in the lanthanide distribution (La/Yb = 70–1000), high Ba (3–20% BaO), association of barite-fluocarbonate, presence of Eu^{2+}-activated apatite, Eu^{2+}-activated strontianite and Fe^{3+}-activated Ca-free albite, all strongly support a carbonatite classification.

It is proposed that fluorapatite was formed during at least two periods: an early generation of REE-rich fluorapatite in sites 1 and 2, and a later generation of REE-poor fluorapatite in sites 3 and 4. The Nd impoverishment (with respect to Ce and La) in fluorapatite from sites 3 and 4 is counterbalanced by Nd enrichment in REE fluocarbonates, so that the rare-earth distribution in the four occurrences remains about the same. However, the concentration of REE in the whole rock is greatly increased at sites 3 and 4.

The ratio La/Nd in fluocarbonates (1.3 to 2.0) is in better agreement with hydrothermal parisite (0.58 to 2.00, ave. 1.26) than igneous, carbonatitic parisite (2.20 to 4.21, ave. 2.84; 14 analyses considered by Fleischer 1978). Fleischer's data also suggest that relative enrichment of La in igneous carbonatite may be general for minerals of the bastnaesite group.

It is tempting to speculate that apatite at sites 1, 2, 5 and 6 is "primary", and that apatite from sites 3 and 4 has been leached by the action of carbonated water leading to REE fluocarbonates according to reactions of the type: REE fluorapatite + $CO_2 \rightarrow$ REE-free fluorapatite + REE fluocarbonate.

Rare-earth patterns and Sr content in apatite from fenite (sites 5 and 6) are similar to those from the Gatineau carbonatites (especially those of site 2). In fact there is nothing in the chemical composition of this mineral to suggest a different origin for the two rock types. An early generation of apatite in fenite is in accord with the conclusion of Heinrich (1966, p. 76) that most fenitization is early in the development of carbonatite complexes.

The calcite–dolomite geothermometer of Powell et al. (1984) suggests equilibration temperatures of 240–300°C for carbonates of the lens-shaped carbonatites. Coexisting pairs yield equilibration temperatures of 240±5°C for sample G (calcite G–dolomite G(2)) and 300±5°C for sample H. The calcite–dolomite pair in sample D yields temperatures of 225±10°C but equilibrium is suspect due to the high content of Sr in dolomite. Calcite coexisting with dolomite (not analyzed) in sample E gives a temperature of 300°C.

The association dolomite–quartz in site 3 also suggests low temperature, and lack of talc, tremolite or diopside, and associated carbonated fluid. An intimate specularite–rutile association (sites 4, 5, 6) suggests extreme oxidation. The rocks would seem to belong to the category of "late carbonatites" (Kapustin 1980, p. 60) or carbonatites formed hydrothermally at 100–300°C (Borodin and Kapustin 1968).

The rock collected at site 3 differs somewhat from the other Gatineau carbonatites: quartz and microcline are the only silicates present and apatite contains little Sr. Fenites do not seem to contain the characteristic alkali silicates of the carbonatites, such as phlogopite, aegirine and Na-amphibole. Possibly this deposit was formed at a very late stage, after silica activity was reduced and fenitization subsided.

Faults, or tension fractures associated with faults, of the Ottawa-Bonnechere rift structure may have provided conduits for REE-bearing hydrothermal solutions during mantle devolatilization in late Precambrian time, and apatite, calcite, dolomite, barite and silicates were deposited under low-to-moderate-temperature, highly oxidizing con-

ditions (sites 1 and 2). These early carbonatites were accompanied or preceded by fenitization (sites 5 and 6). Later reworking of carbonatites and fenites by low-temperature solutions, possibly connected with waning Grenvillian metamorphism, resulted in formation of secondary apatite and REE fluocarbonates in carbonatite (site 4) and, perhaps, monazite (site 5), and the introduction of additional lanthanides. A late stage in this process resulted in leaching, transportation and redeposition of REE and P in a new location (site 3), thus accounting for mineralogical differences and absence of a typical fenite association.

Acknowledgments

References

Åmli, R. and Griffin, W. L. (1975) Microprobe analysis of REE minerals using empirical correction factors. American Mineralogist, 60, 599–606.

Borodin, L. S. and Kapustin, Yu. L. (1968) Carbonatite rare-element deposits. In K. A. Vlasov, Ed., Geochemistry and Mineralogy of Rare Elements and Genetic Types of their Deposits, Vol. 3: Genetic types of Rare-element Deposits, p. 197–241. Israel Program for Scientific Translations, Jerusalem.

Drake, M. J. and Weill, D. F. (1972) New rare earth element standards for electron microprobe analysis. Chemical Geology, 10, 179–181.

Fleischer, M. (1978) Relative proportions of the lanthanides in minerals of the bastnaesite group. Canadian Mineralogist, 16, 361–363.

Fleischer, M. and Altschuler, Z. S. (1969) The relationship of the rare-earth composition of minerals to geological environment. Geochimica et Cosmochimica Acta, 33, 725–732.

Garson, M. S., Coats, J. S., Rock, N. M. S., and Deans, T. (1984) Fenites, breccia dykes, albitites, and carbonatitic veins near the Great Glen Fault, Inverness, Scotland. Journal of the Geological Society of London, 141, 711–732.

Haskin, L. A., Haskin, M. A., Frey, F. A., and Wildeman, T. R. (1968) Relative and absolute terrestrial abundances of the rare earths. In E. Ingerson, Ed., Origin and distribution of the elements, p. 889–912. Pergamon Press, Oxford.

Heinrich, E. W. (1966) The Geology of Carbonatites. Rand McNally, Chicago.

Hogarth, D. D. (1981) Partie ouest de la région de Quinnville. Québec, Ministère de l'énergie et des ressources, DPV-816.

Hogarth, D. D. and Lapointe, P. (1984) Amphibole and pyroxene development in fenite from Cantley, Quebec. Canadian Mineralogist, 22, 281–295.

Kapustin, Yu L. (1980) Mineralogy of Carbonatites. Published for The Smithsonian Institution and The National Science Foundation by Amerind Publishing Co., New Delhi.

Kumarapeli, P. S. and Saull, V. A. (1966) The St. Lawrence Valley System: a North American equivalent of the East African Rift Valley System. Canadian Journal of Earth Sciences, 3, 639–658.

Lumbers, S. B. (1978) Geological setting of alkalic rock-carbonatite complexes in eastern Canada. In J. C. Braga, Ed., Proceedings of the First International Symposium on Carbonatites, p. 81–89. Ministério das Minas e Energia, Departmento Naciona da Prodµcão Mineral, Pµcos de Caldas.

Mariano, A. N. (1978) The application of cathodoluminescence for carbonatite exploration and characterization. In J. C. Braga, Ed., Proceedings of the First International Symposium on Carbonatites, p. 39–57. Ministério das Minas e Energia, Departamento Nacional da Prodµcão Mineral, Pµcos de Caldas.

Mariano, A. N. and Ring, P. J. (1975) Europium-activated cathodoluminescence in minerals. Geochimica et Cosmochimica Acta, 39, 649–660.

Powell, R., Condliffe, D. M. and Condliffe, E. (1984) Calcite-dolomite geothermometry in the system $CaCO_3$–$MgCO_3$–$FeCO_3$: an experimental study. Journal of Metamorphic Geology, 2, 33–41.

Rucklidge, J. C. and Gasparrini, E. L. (1969) Specifications of a computer program for processing electron microprobe data: EMPADR VII. Department of Geology, University of Toronto, Toronto, Canada.

Samoylov, V. S. and Smirnova, Ye. V. (1980) Rare-earth behaviour in carbonatite formation and the origin of carbonatites. Geochemistry International, 17, (6), 140–152.

Shannon, R. D. (1976) Revised effective ionic radii and systematic studies of interatomic distances in halides and chalcogenides. Acta Crystallographica, A32, 751–767.

Shaw, D. M., Dostal, J. and Keays, R. R. (1976) Additional estimates of continental surface Precambrian Shield composition in Canada. Geochimica et Cosmochimica Acta, 40, 73–83.

Solberg, T. N. (1982) Fluorine electron microprobe analysis: variations of the X-ray peak shape. In K. F. J. Heinrich, Ed., Microbeam Analysis–1982, p. 148–150. San Francisco Press, San Francisco.

Solberg, T. N. and Speer, J. A. (1982) QALL, a 16 element analytical scheme for efficient petrologic work on an automated ARL-SEMQ: application to mica reference samples. In K. F. J. Heinrich, Ed., Microbeam Analysis–1982, p. 422–426. San Francisco Press, San Francisco.

Speer, J. A. and Solberg, T. N. (1982) Rare earth pyrosilicates ($RE_2Si_2O_7$) as potential electron microprobe standards. In K. F. J. Heinrich, Ed., Microbeam Analysis–1982, p. 445–446. San Francisco Press, San Francisco.

Wayne, D. M. (1984) Electron microprobe analysis of rare-earth-element-bearing phases from the White Cloud pegmatite, South Platte district, Jefferson County, Colorado. M.Sc. Thesis, Department of Earth Sciences, University of New Orleans, New Orleans.